

Hence, this work was aimed to develop a finite element model with incorporation of phase change during dehydration of mushroom in a cabinet–air–dryer to study the temperature and moisture profiles inside the mushroom.

Experimental details

Freshly harvested white button mushrooms were purchased from the local greengrocers. They were sorted manually based on shape, size and color before processing. Dimensionally similar mushroom were selected for the experiments. The dimension of these mushrooms was calculated using vernier calipers (Forbes) with an accuracy of 0.02 mm. All the mushrooms were washed thoroughly to remove soil impurities. Two mushrooms viz. sample 1 (S1) and sample 2 (S2) of approximately same dimensions and weight were chosen. The selected samples were then placed in a cabinet–air–dryer (Industrial & laboratory tools corporation, Chennai Serial No. S1016), dried at a temperature of 54±1°C. Mushroom S1 was analyzed for moisture content, S2 for temperature profile. Figure 1 shows the schematic arrangement of the experimental setup.

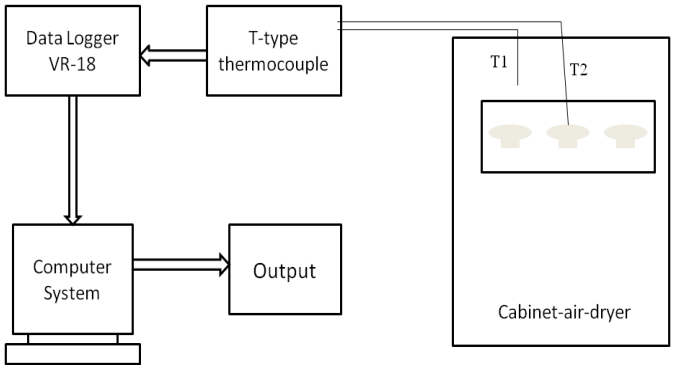

Figure 1 Schematic arrangement of the experimental setup.

Moisture content analysis

The initial weight of the mushroom S1 was measured before placing it into the dryer maintained at 54±1°C and at regular intervals of 30minutes mushroom was weighed on an electronic balance (Contech CA–123). Drying was carried out for a period of 5hours. To determine the bone dry weight of mushroom S1, it was put inside a hot air oven maintained at 100°C to dry overnight (16hours). The bone dry weight of the sample was measured and used to calculate the initial moisture content on dry basis (gram H_2O/gram dry weight).

Temperature profile determination

Temperature inside the mushroom S2 was measured using two calibrated T–type thermocouples. One thermocouple was inserted in the geometric centre of the mushroom head portion and another at the geometric centre of the stem of mushroom. The temperature inside the cabinet was monitored using T–type thermocouple, which was placed very close to the mushroom. All the thermocouples were connected to the data logger (VR–18, Brainchild Electronics Co. Ltd.) and recorded at regular intervals of 30s throughout the drying process.

Modeling formulations

This model is based on the following assumptions: (i) shrinkage is negligible; (ii) material properties such as specific heat, thermal conductivity and porosity are constant, and (iii) material is isotropic.

Governing equations

Heat balance equation:

$$\rho C_p \frac{\partial T}{\partial t} = \nabla.\left(k \nabla T\right) \quad (1)$$

Where, ρ– Density (kg/m^3); C_p – Specific heat (J/kg K); T–Temperature (K)

Mass balance equation:

$$\frac{\partial W}{\partial t} = \nabla.(D \nabla W) \quad (2)$$

Where, W–Water content (kg/kg); D–Water (liquid or vapor) diffusion coefficient of mushroom (m^2/s)

Boundary conditions for heat and mass transfer

Figure 2 shows the geometry of mushroom and the meshed geometry (consisting of 9936 elements), respectively. Mushroom was placed on a stainless steel plate during the experiment. Heat transfer at the top and lateral surfaces (external) by convection is balanced with internal conduction heating. Hence, the corresponding boundary condition for equation (1) is given by Wang & Brennan[6] follows:

$$-k \nabla T = L_v D \rho \nabla W + h(T_S - T_{amb}) \quad (3)$$

Where, k–Thermal conductivity (W/m·K); T–Temperature (K); D–Water (liquid or vapor) diffusion coefficient of mushroom (m^2/s); ρ- Density (kg/m^3); W–Water content (kg/kg); S–solid or surface

$L_v D \rho \nabla W$ denotes the quantity of heat required to evaporate the moisture through unit area. Moisture transport through mushroom surface is balanced by convective flux as given by the equation below,

$$-D \rho_B \nabla W = K_g (P_S - P_{amb}) \quad (4)$$

Where, $P_S = a_w P_{sat}\left(T_S\right)$ and $P_{amb} = (RH/100).P_{sat}\left(T_{amb}\right)$ K_g– Mass transfer coefficient

Equations for $P_{sat}\left(T_{amb}\right)$ and $P_{sat}\left(T_{amb}\right)$ were taken from Zanoni et al.[10] and a_w is defined from Combs (2004). Density (ρ) of mushroom increases with the decrease in moisture content. Hence, it was included as a function of moisture content. The data for variation of density with change in moisture content was taken from Boukouvalas et al.[11] Effective moisture diffusivity (D) for mushroom was given as 5.065x10^{-9}m^{2}s^{-1}.[12] Thermo–physical properties of mushroom such as specific heat and thermal conductivity were given as a constant. Lespinard et al.[9] proposed the specific heat (C_p) as 3883J Kg^{-1}°C and thermal conductivity (k) of mushroom as 0.4324W m^{-1}°C.

Heat transfer coefficient (h_L) was included in the model using the following expression.[13]

$$N_{Sh} = \frac{K_g \times dia}{D} = [4 + 1.21(N\,\mathrm{Re} \times NSc)^{0.67}]^{0.5} \quad (5)$$

where, dia is the diameter of the mushroom head portion in meters. Prandtl number (N_{Pr}) was determined taking into consideration the standard thermal properties of air at 54°C.

Mass transfer coefficient (K_g) governs the rate of moisture transfer from the mushroom to the free air stream. It was included in the model with the help of Sherwood number (N_{Sh}). The head of the mushroom is spherical and due to its large size, it will determine the overall rate of

Citation: Choudhary A, Gopirajah R, Anandharamakrishnan C. Computational modeling of dehydration of mushroom. *MOJ Food Process Technol.* 2018;6(3):264–270. DOI: 10.15406/mojfpt.2018.06.00174

mass transfer. Hence, Sherwood number was calculated by assuming mushroom as a sphere under forced convection (Perry's Chemical Engineers' Handbook).

$$N_{Sh} = \frac{K_g \times dia}{D} = [4 + 1.21(N\,\mathrm{Re} \times NSc)^{0.67}]^{0.5} \quad (6)$$

Schmidt number (N_{Sc}) was incorporated as the ratio of dynamic viscosity to that of kinematic viscosity of air at 54°C.

A mass transfer co–efficient correction factor was incorporated in the model as,

$$K_g = K_{gc} \times 1.652 \times 10^{-2} \quad (7)$$

Dell workstation T5400 was used for running the finite element model simulation. Drying process simulation was carried out for 18000s.

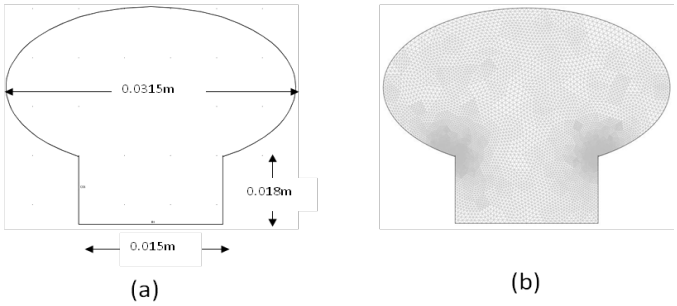

Figure 2 (a) Geometry. (b) Meshed geometry.

Results and discussion

The geometry of mushroom is axis–symmetric, therefore it can be said that the two and three–dimension model are equivalent with respect to shape and the transport phenomenon occurring. Moreover, the calculation time of the two–dimensional domain will be much lower than the three–dimensional domain.[9]

Experimental validation of the model at 55°C (case A)

The simulation predictions were compared with the experimental measurements of temperatures for mushroom drying process. The simulation results were in good agreement with the experimental results as shown in Figure 3. Initially, there is a high temperature gradient (ΔT) between the mushroom and air temperature due to which the rate of heat transfer to the mushroom is very high. As a result, steep rise in temperature of mushroom was observed initially, followed by steady state condition after 6600s temperature. The difference in experimental and modeled temperature profile can be attributed to the combined effects of experimental and model assumptions viz., shrinkage is negligible, isotropic condition and thermal properties of materials.

Balaban[8] compared the effect of incorporation of shrinkage in food materials during drying and concluded that non consideration of shrinkage in simultaneous heat and mass transfer models can cause significant differences between the actual values of temperature and the results as predicted by the model. The same could be seen in this model. However, it was observed that as the time progresses the experimental temperature slowly approaches the modeled temperature thereby reducing the difference in modeled and experimental values. Ranjan et al.[14] predicted drying behavior of banana by varying drying air temperature using finite element model without considering shrinkage effects, which resulted in good agreement with the experimental results.

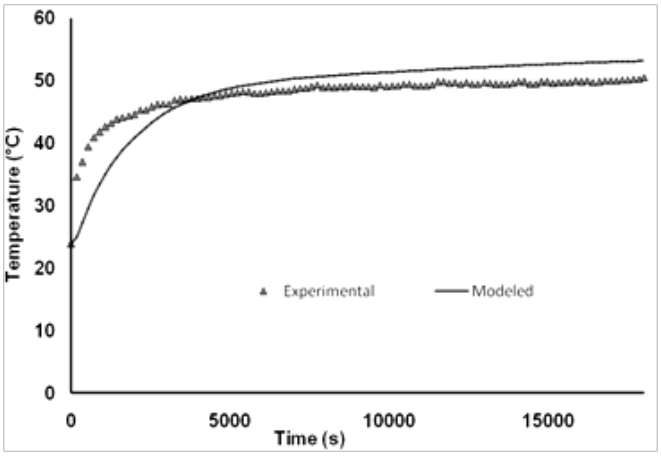

Figure 3 Validation of experimental and modeled temperature.

Figure 4 shows the variation of temperature with respect to time along five different points (as depicted points in Figure). It can be seen that the rise in temperature along all these points is almost the same. The temperature at points S1 and S2 are located in the stem of the mushroom and rises steeply. Heat transfer is inversely proportional to the surface area and the surface area of the head is more than that of the stem. Therefore, transfer of heat to the stem took place at a much faster rate than the mushroom head portion. This observation was same as reported earlier by Senadeera et al.[15] that as the surface area increases, drying rate decreased at every drying temperature. The points H1 and H3 also show a steep rise due to their proximity to the boundary surface of the mushroom. However, H2 located at the centre of mushroom shows a gradual increase in temperature.

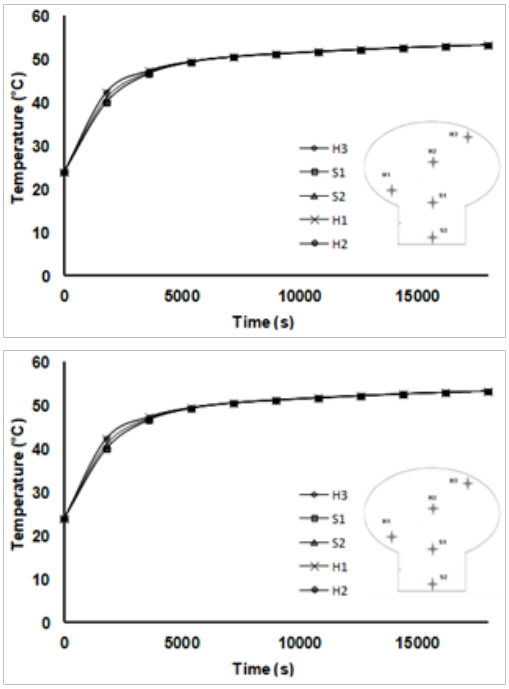

Figure 4 Variation of temperature along different points as depicted.

Citation: Choudhary A, Gopirajah R, Anandharamakrishnan C. Computational modeling of dehydration of mushroom. *MOJ Food Process Technol.* 2018;6(3):264–271. DOI: 10.15406/mojfpt.2018.06.00174

Figure 5 shows that the predicted moisture content profiles are in close agreements with the experimental measurements. This clearly indicates that the model can be used effectively to predict the reduction in moisture content at different intervals of time during drying process. Figure 6 shows the variation of moisture content during drying at different intervals of time. As the drying time progresses heat penetrates towards the centre of the mushroom. This also results in simultaneous diffusion of moisture from the centre towards the surface of the mushroom.

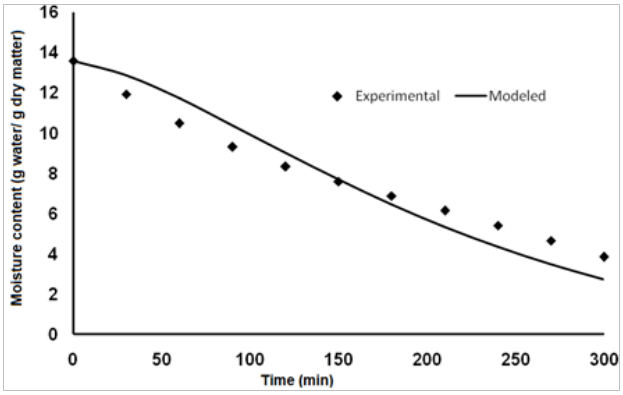

Figure 5 Validation of predicted moisture content profiles with experimental measurements.

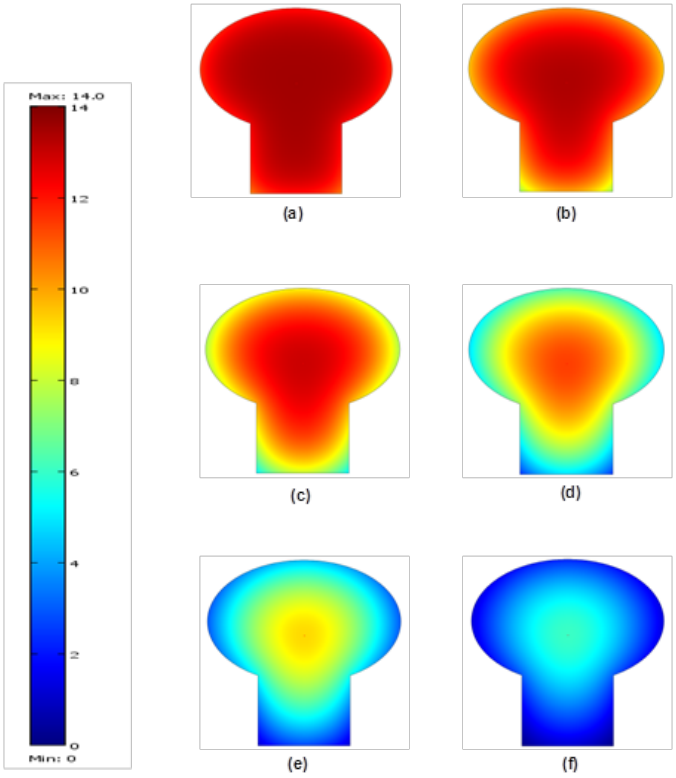

Figure 6 Predicted moisture content profile during drying of mushroom at 55°C with different time intervals of (a) 1800s. (b) 3600s. (c) 7200s. (d) 10800s. (e) 14400s. (f) 18000s.

The slowest heating zone (SHZ) is defined as the region at which food product receives the least amount of heat during thermal processing. Tracking the slow heating zone (SHZ) is important to assess the effectiveness of any process involving heat transfer Padmavathi & Anandharamakrishnan[16] It was observed that the moisture content is highest at the geometric centre of the mushroom head for any time step as it also happens to be the slowest heating zone (SHZ).

The variation of moisture content of mushroom at 5 different points is depicted in Figure 7. From the Figure 7, it can be observed that the rate of drying is minimum at H2 and maximum at H3 as the transfer of moisture from the stem is faster than that of the head portion as mentioned earlier in the case of temperature. Also, it is found that the drying rate is almost the same for points H1 and H3 due to its proximity to the boundary surface. The drying rate is similar for S1 and H2 since S1 is located at the interface of the head and the stem. Thus, it can be concluded that diffusion controls the rate of drying and therefore is the rate limiting step. Since the model has already been validated with case A (T_{wall}=55°C), it can be used to make predictions for drying at different temperatures. In this view, the following two case studies were performed with the same boundary conditions except for wall boundary condition as given below;

- Case B: T_{wall}=45°C
- Case C: T_{wall}=35°C

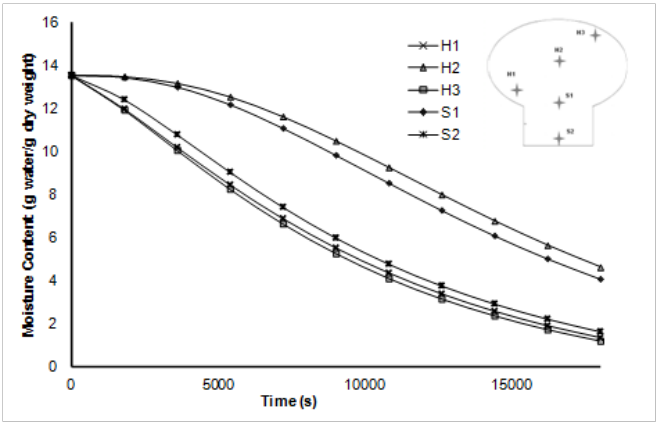

Figure 7 Variation of moisture along different points.

Effect of drying air temperature on drying of mushroom

In this study, effect of two different drying air temperatures (case B and case C) during drying were compared with case A. Figure 8 shows the variation of temperature profile for drying the product under conditions of Case A, Case B and Case C. It can be observed that in case A, the product temperature reaches close to the ambient temperature. However, the difference in temperature of the product and the surrounding is maximum for case C during the same drying period. From this it can be observed that the rate of heat transfer is directly proportional to the temperature gradient (ΔT) across the boundary of mushroom. In Case A, the duration at which temperature reaches steady state condition is found to be less when compared to case B and Case C dried at lower temperatures. This is due to the fact that increase in air temperature increases the drying rate by improving evaporation rate with necessary heat of vaporization. Decreasing the drying air temperature gradually with respect to decrease in moisture content will result in maintaining constant evaporation rate throughout the process.[17] Steady–state increase in temperature during

drying at Case A, Case B, Case C begins after 6000s, 4200s and 2400s of drying time, respectively. Hence, Case A is considered to be more appropriate since the temperature of drying air should be quite high to remove the high moisture content in the product initially.

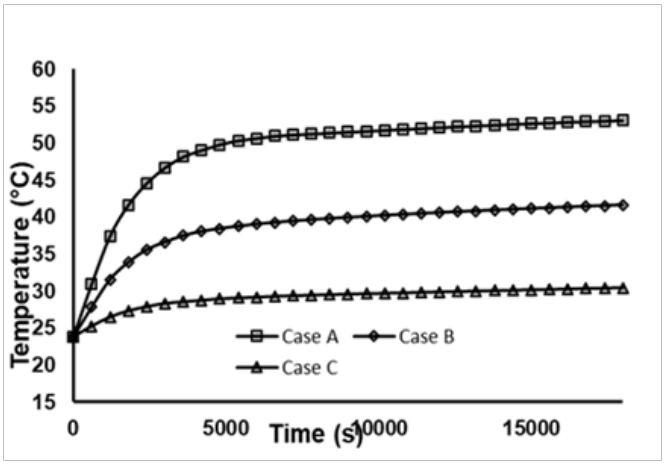

Figure 8 Temperature Profile for different drying temperatures of 55°C (Case A), 45°C (Case B), and 35°C (Case C).

The temperature and moisture profiles obtained above are comparable with the results of Ranjan et al.[14] and it was found that there is not much significant difference in the trend of moisture profiles. Their model shows good agreement with the experimental results without considering shrinkage effects. Similar results were also observed when analyzing the drying behavior in various other vegetables such as carrot, garlic, onion, potato etc.[18,19]

Figure 9 gives the moisture profile for drying under case A, case B and case C. In case A, due to the lower relative humidity of air, partial vapor pressure of drying air becomes low which results in increased moisture evaporation rate.[17] This indicates that, as the drying temperature increases, the rate of removal of moisture from the product also increases. The final moisture content after 18000s of drying as predicted by the model for drying temperatures of case A, case B and case C are 3.32, 6.49 and 9.51gram of water per gram dry matter, respectively. Thus, it can be concluded that the rate of drying is highly controlled by temperature of drying during the process.

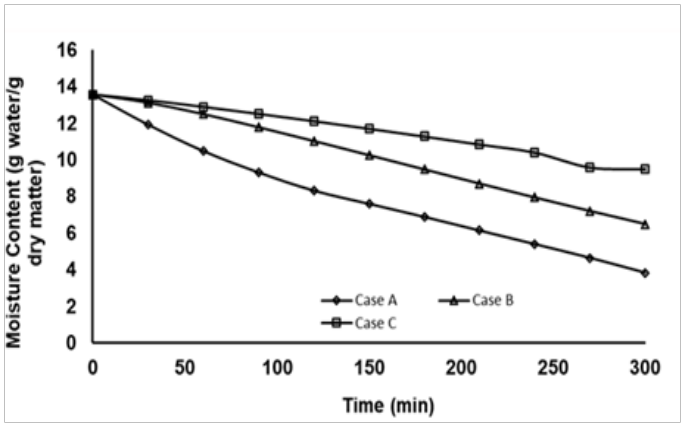

Figure 9 Moisture content profile for drying at different temperatures of 55°C (Case A), 45°C (Case B), and 35°C (Case C).

Effect of moisture variations along axial and radial direction

To study the variation of moisture within the mushroom along the radial as well as the axial direction, Moisture profiles were plotted for all the three cases (case A, case B and case C) with 3 different time steps.

Radial direction

Moisture profiles were plotted along the radial direction through the head of the mushroom as shown in Fig. 10. The variation of moisture content at various time intervals of 60s, 600s, and 6000s with respect to Case A, case B and case C are shown in Figure 10 respectively. The figure shows that at 60s of drying, there is no considerable reduction in moisture content. But after 600 s of drying a small reduction in moisture content to around 13%db from 13.5%db was observed in all the cases at the boundary surface, and there was no reduction from the core of the mushroom. Further, after 6000s of drying the moisture level drops drastically to 7% db in Case A, 9.9%db in case B and 11.4% in case C at the boundary surface and also the moisture content inside the mushroom reduces due to the diffusion of moisture towards the surface. Thus, significant reduction in moisture content takes place after 600s of drying and increases from mushroom surface to the inner core.

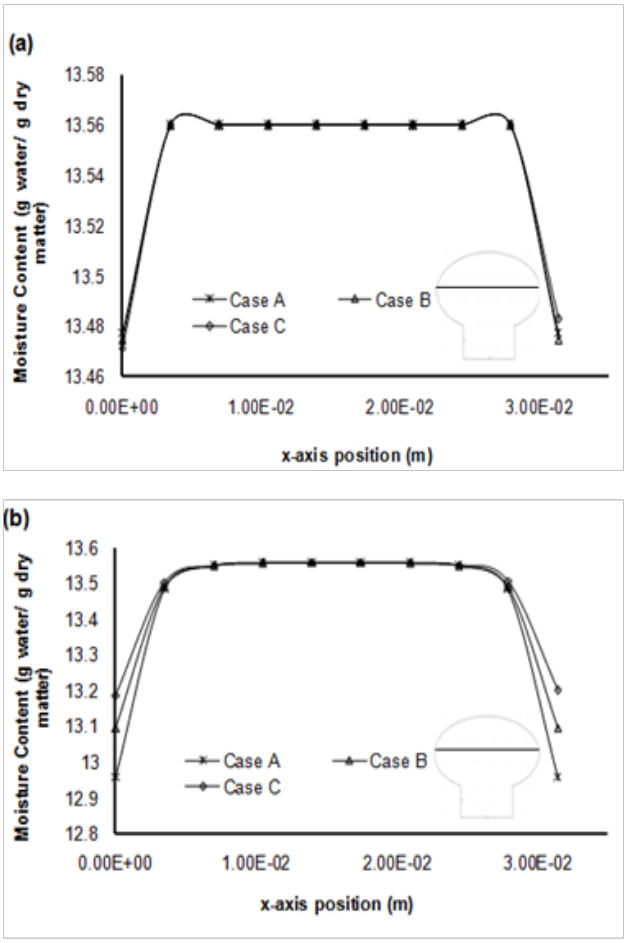

Citation: Choudhary A, Gopirajah R, Anandharamakrishnan C. Computational modeling of dehydration of mushroom. *MOJ Food Process Technol.* 2018;6(3):264–271. DOI: 10.15406/mojfpt.2018.06.00174

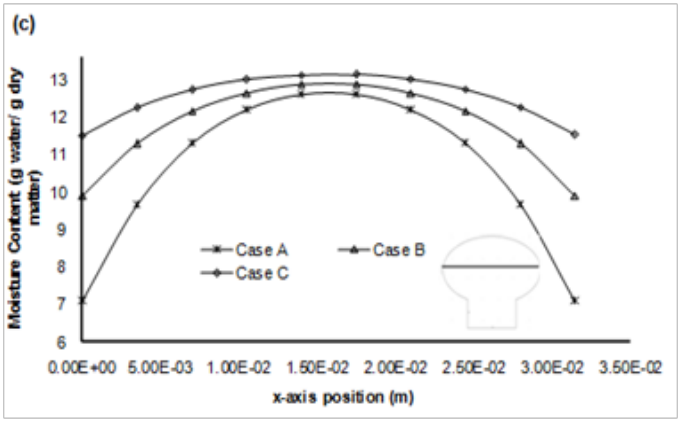

Figure 10 Moisture variation within mushroom along radial direction after (a) 60s. (b) 600s. (c) 6000s at different drying temperatures of 55°C (Case A), 45°C (Case B), and 35°C (Case C).

Axial direction

Figure 11 demonstrates the variation of moisture content along the axial direction which pass through the head and stem of the mushroom for different drying temperatures (case A, case B, case C) at various time intervals of 60s, 600s and 6000s, respectively. The negative y–axis indicate the stem of the mushroom.

At 60s of drying (Figure 11A) there is no considerable reduction in moisture content at the stem and head portions. After 600s of drying, stem showed slightly higher moisture content than head portion. However, Figure 11C indicates that after 6000s of drying the moisture content of the stem is lesser than that of the head for all the cases. Further, it can be observed that the amount of moisture increases from the surface to the core of mushroom.

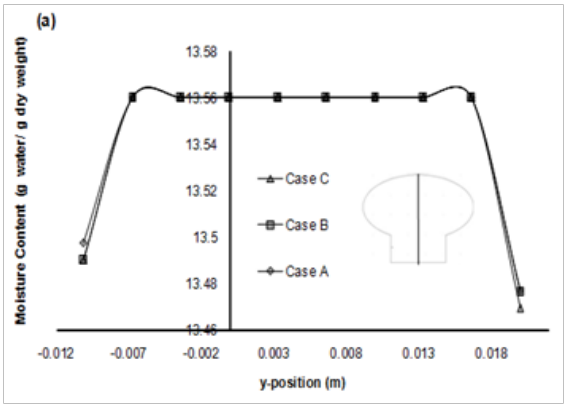

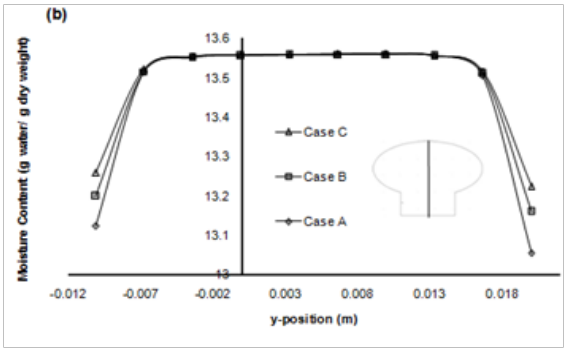

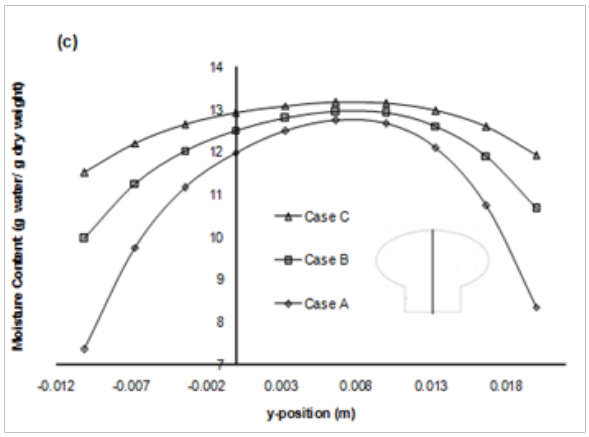

Figure 11 Moisture variation within mushroom along axial direction after (a) 60s. (b) 600s. (c) 6000s at different drying temperatures of 55°C (Case A), 45°C (Case B), and 35°C (Case C).

Conclusion

A two–dimensional finite element model was developed considering simultaneous heat and mass transfer for predicting moisture content during dehydration of mushroom. The phase change mechanism was incorporated in the model. Various factors, such as, heat transfer coefficient, mass transfer coefficient, water activity of the mushroom, specific heat, thermal conductivity, and diffusion coefficient, etc., were incorporated into the model for better predictions of transport processes. The developed model was validated with the experimental measurements of temperature and moisture content. The model was extended to investigate the moisture content variation and temperature profile for different temperatures (35°C, 45°C). The temperature profile for increase in temperature showed that the rise in temperature is directly proportional to the difference in temperature between the product and the surrounding (ΔT). It was found that for drying at 35°C, 45°C, 55°C steady–state increase in temperature begins after 2400s, 4200s, and 6000s of drying time, respectively. Also, after 5hours of drying, maximum loss of moisture was obtained when drying at 55°C and the lowest loss of moisture was found in 35°C. Final moisture content after 35°C, 45°C and 55°C was 9.51, 6.49, 3.32gram water/gram dry matter, respectively. Thus, the developed model was used to determine the processing time of mushroom at different temperatures (35°C, 45°C, 55°C) for long term storage depending upon the usage. This model can be extended to other vegetables and can help in predicting the temperature and moisture profile of the product and thus help in producing processed food of highest quality.

Acknowledgements

The authors thank the Director, CSIR-CFTRI for providing the lab facility and support for conducting this research.

Conflict of interest

The authors declare that there is no conflict of interest.

References

1. Erik Torringa, Erik Esveld, Ischa Scheewe, et al. Osmotic dehydration as a pre–treatment before combined microwave–hot–air drying of mushrooms. *J Food Eng*. 2001;49(2–3):185–191.

2. Rama V, John PJ. Effects of methods of drying and pretreatments on quality of dehydrated mushroom. *Indian Food Pack*. 2000;54:59–64.
3. Giri SK, Prasad S. Drying kinetics and rehydration characteristics of microwave–vacuum and convective hot–air dried mushrooms. *J Food Eng*. 2007;78(2):512–521.
4. Walde SG, Velu V, Jyothirmayi T, et al. Effects of pretreatments and drying methods on dehydration of mushroom. *J Food Eng*. 2006;74(1):108–115.
5. Ghiaus AG, Margaris DP, Papanikas DG, et al. Mathematical Modeling of the Convective Drying of Fruits and Vegetables. *J Food Sci*. 1997;62(6):1154–1157.
6. Wang N, Brennan JG. A mathematical model of simultaneous heat and moisture transfer during drying of potato. *J Food Eng*. 1995;24(1):47–60.
7. Balaban M, Pigott G. Mathematical Model of Simultaneous Heat and Mass Transfer in Food with Dimensional Changes and Variable Transport Parameters. *J Food Sci*. 1988;53(3):935–939.
8. Balaban M. Effect of Volume Change in Foods on The Temperature and Moisture Content Predictions of Simultaneous Heat and Moisture Transfer Models. *J Food Process Eng*. 1990;12(1):67–88.
9. Lespinard AR, Goñi SM, Salgado PR, et al. Experimental determination and modelling of size variation, heat transfer and quality indexes during mushroom blanching. *J Food Eng*. 2009;92:8–17.
10. Zanoni B, Peri C, Gianotti R. Determination of the thermal diffusivity of bread as a function of porosity. *J Food Eng*. 1995;26(4):497–510.
11. Boukouvalas CJ, Bisharat GI, Krokida MK. Structural Properties of Vegetables During Air Drying. *Int J Food Prop*. 2010;13(6):1393–1404.
12. Murumkar RP, Jain SK, Pilaskar PS, et al. Osmo–Fluid Bed Drying of White Button Mushroom. *Bioved–An International Bi–Annual Journal of Life Science*. 2007;18:47–52.
13. Yang H, Sakai N, Watanabe M. Drying Model with Non–Isotropic Shrinkage Deformation Undergoing Simultaneous Heat and Mass Transfer. *Dry Technol*. 2001;19(7):1441–1460.
14. Ranjan R, Irudayaraj J, Reddy JN, et al. Finite–Element Simulation and Validation of Stepwise Drying of Bananas. *Numer Heat Transf Part Appl*. 2001;45(10):997–1012.
15. Senadeera W, Bhandari BR, Young G, et al. Influence of shapes of selected vegetable materials on drying kinetics during fluidized bed drying. *J Food Eng*. 2003;58(3):277–283.
16. Padmavati R, Anandharamakrishnan C. Computational Fluid Dynamics Modeling of the Thermal Processing of Canned Pineapple Slices and Titbits. *Food Bioprocess Technol*. 2013;6(4):882–895.
17. Islam MR, Ho JC, Mujumdar AS. Convective Drying with Time–Varying Heat Input: Simulation Results. *Dry Technol*. 2003;21(7):1333–1356.
18. Souraki BA, Andrés A, Mowla D. Mathematical modeling of microwave–assisted inert medium fluidized bed drying of cylindrical carrot samples. *Chem Eng Process Process Intensif*. 2009;48(1):296–305.
19. Krokida MK, Karathanos VT, Maroulis ZB, et al. Drying kinetics of some vegetables. *J Food Eng*. 2003;59(4):391–403.

Citation: Choudhary A, Gopirajah R, Anandharamakrishnan C. Computational modeling of dehydration of mushroom. *MOJ Food Process Technol.* 2018;6(3):264–271. DOI: 10.15406/mojfpt.2018.06.00174